Available online at www.sciencedirect.com
ScienceDirect
Nuclear Medicine and Biology 38 (2011) 19–28
NUCLEAR MEDICINE AND BIOLOGY
www.elsevier.com/locate/nucmedbio

Radiolabeling of rituximab with ^{188}Re and ^{99m}Tc using the tricarbonyl technology

Carla Roberta Dias[a], Simone Jeger[b], João Alberto Osso Jr [a], Cristina Müller[b], Christine De Pasquale[b], Alexander Hohn[b], Robert Waibel[b], Roger Schibli[b,c,*]

[a]*Instituto de Pesquisas Energéticas e Nucleares, Av. Professor Lineu Prestes 2242, 05508-000 São Paulo, Brazil*
[b]*Center for Radiopharmaceutical Sciences ETH-PSI-USZ, Paul Scherrer Institute, 5232 Villigen-PSI, Switzerland*
[c]*Department of Chemistry and Applied Biosciences of the ETH, 8093 Zurich, Switzerland*

Received 16 March 2010; received in revised form 9 May 2010; accepted 14 May 2010

Abstract

Introduction: The most successful clinical studies of immunotherapy in patients with non-Hodgkin's lymphoma (NHL) use the antibody rituximab (RTX) targeting CD20$^+$ B-cell tumors. Rituximab radiolabeled with β^- emitters could potentiate the therapeutic efficacy of the antibody by virtue of the particle radiation. Here, we report on a direct radiolabeling approach of rituximab with the ^{99m}Tc- and ^{188}Re-tricarbonyl core (IsoLink technology).

Methods: The native format of the antibody (RTX_{wt}) as well as a reduced form (RTX_{red}) was labeled with $^{99m}Tc/^{188}Re(CO)_3$. The partial reduction of the disulfide bonds to produce free sulfhydryl groups (–SH) was achieved with 2-mercaptoethanol. Radiolabeling efficiency, in vitro human plasma stability as well as transchelation toward cysteine and histidine was investigated. The immunoreactivity and binding affinity were determined on Ramos and/or Raji cells expressing CD20. Biodistribution was performed in mice bearing subcutaneous Ramos lymphoma xenografts.

Results: The radiolabeling efficiency and kinetics of RTX_{red} were superior to that of RTX_{wt} (^{99m}Tc: 98% after 3 h for RTX_{red} vs. 70% after 24 h for RTX_{wt}). $^{99m}Tc(CO)_3$-RTX_{red} was used without purification for in vitro and in vivo studies whereas $^{188}Re(CO)_3$-RTX_{red} was purified to eliminate free ^{188}Re-precursor. Both radioimmunoconjugates were stable in human plasma for 24 h at 37°C. In contrast, displacement experiments with excess cysteine/histidine showed significant transchelation in the case of $^{99m}Tc(CO)_3$-RTX_{red} but not with pre-purified $^{188}Re(CO)_3$-RTX_{red}. Both conjugates revealed high binding affinity to the CD20 antigen (K_d=5–6 nM). Tumor uptake of $^{188}Re(CO)_3$-RTX_{red} was 2.5 %ID/g and 0.8 %ID/g for $^{99m}Tc(CO)_3$-RTX_{red} 48 h after injection. The values for other organs and tissues were similar for both compounds, for example the tumor-to-blood and tumor-to-liver ratios were 0.4 and 0.3 for $^{99m}Tc(CO)_3$-RTX_{red} and for $^{188}Re(CO)_3$-RTX_{red} 0.5 and 0.5 (24 h pi).

Conclusion: Rituximab could be directly and stably labeled with the matched pair $^{99m}Tc/^{188}Re$ using the IsoLink technology under retention of the biological activity. Labeling kinetics and yields need further improvement for potential routine application in radioimmunodiagnosis and therapy.
© 2011 Elsevier Inc. All rights reserved.

Keywords: Rituximab; ^{188}Re; ^{99m}Tc; Tricarbonyl core; Radioimmunoconjugate

1. Introduction

The investigation of novel tumor-targeting radiopharmaceuticals is currently one of the potential fields of interest for researchers for both tumor scintigraphy and/or treatment. Radiolabeled antibodies are important clinical reagents for both tumor imaging and therapy and also for providing an effective evaluation of the pharmacokinetics [1]. Monoclonal antibodies (mAb) have significantly contributed to the success in the treatment of hematological malignancies. Radioimmunotherapy (RIT) is advantageous compared to unlabeled therapeutic antibodies, given the additive effect of radiation-induced cytotoxicity and the ability of the associated radioactivity to kill tumor cells distant from the

* Corresponding author. Institute for Pharmaceutical Sciences, ETH Hönggerberg, HCI H425, Wolfgang-Pauli-Strasse 10, 8093 Zurich, Switzerland. Tel.: +41 56 310 2837; fax: +41 56 310 2849.
E-mail addresses: roger.schibli@psi.ch, roger.schibli@pharma.ethz.ch (R. Schibli).

0969-8051/$ – see front matter © 2011 Elsevier Inc. All rights reserved.
doi:10.1016/j.nucmedbio.2010.05.010

bound radiolabeled antibody [2]. In 2002, yttrium-90 ibritumomab tiuxetan (Zevalin; Biogen Idec, Inc., Cambridge, MA, USA) became the first radioimmunotherapeutic agent approved by the FDA. In 2003, iodine-131 tositumomab (Bexxar; Corixa Corp, Seattle, WA, USA) received approval by the FDA. Both compounds are used for the treatment of patients with non-Hodgkin's lymphoma (NHL) [3–5].

Rituximab (RTX), the human IgG1-type chimeric form of the parent murine antibody ibritumomab, is specifically targeted against CD20, a surface antigen expressed by pre-B and mature human B lymphocytes, by >90% of B-cell NHLs, but not by hematopoietic stem cells, pro-B cells, normal plasma cells or other normal tissues [6–9]. Binding affinity of rituximab to CD20 is approximately 5 nM [10]. There is strong evidence that apoptosis, cell-mediated cytotoxicity, complement-dependent cell lysis and cytokine release are primarily responsible for the therapeutic effect of rituximab [7,11].

A number of methods have been proposed for labeling proteins in general and antibodies in particular. ^{99m}Technetium (^{99m}Tc) and ^{188}Rhenium (^{188}Re) represent an attractive pair of radionuclides for biomedical use because of their favorable decay properties for diagnosis (^{99m}Tc: 6 h half-life, 140-keV γ-radiation) and therapy (^{188}Re: 17 h half-life, 2.12-MeV β^-_{max} radiation) and also due to their onsite availability through the use of ^{99}Mo/^{99m}Tc and ^{188}W/^{188}Re generator systems. ^{188}Re and ^{99m}Tc can be conjugated to antibodies using similar chemistry methods [12]. Ferro-Flores et al. [13] have recently described the development of a freeze-dried kit formulation for the instant preparation of a ^{188}Re-labeled anti-CD20 mAb. Stopar et al. [14] published a study on the radiolabeling of RTX with ^{99m}Tc. Furthermore, Torres-García et al. [15] published preliminary studies on the biokinetics of a ^{188}Re-labeled anti-CD20 mAb in patients.

The organometallic fac-$[M(CO)_3]^+$ core (M=^{99m}Tc, ^{188}Re) was introduced for the development of new target-specific radiopharmaceuticals. It has proven to be a versatile synthon for the labeling of different types of bioactive molecules, notably recombinant proteins, peptides and small molecules [16]. The ^{99m}Tc synthon can be readily prepared via a one-step kit formulation (IsoLink, Covidien, Petten, The Netherlands) in high yields. A two-step kit preparation for the ^{188}Re-analog is in development [17]. The $[M(CO)_3]^+$ core (M=^{99m}Tc, ^{188}Re) possesses a high in vivo stability due to the kinetic inertness of the low-valent, organometallic metal core. The relative high chemical stability of the precursors allows radiolabeling under mild, physiological conditions, suitable for the labeling of temperature-sensitive molecules such as proteins. In fact, $[^{99m}Tc(CO)_3]^+$ is readily used for direct labeling of recombinant proteins expressing a 6xHis-tag [18–20]. Most recently, Chen et al. [21] described the radiolabeling of trastuzumab (Herceptin) with $[^{188}Re(CO)_3]^+$. The study shows for the first time that the use of the tricarbonyl core can be a promising and suitable strategy for the radiolabeling of antibodies with ^{188}Re.

In this study, we present the radiolabeling procedure of the commercial anti-CD20 antibody rituximab with $[^{99m}Tc(CO)_3]^+$ and $[^{188}Re(CO)_3]^+$ as a potential alternative to the ^{111}In/^{90}Y-Zevalin system for diagnosis and therapy of NHL. A comparative preclinical evaluation of the in vitro and the in vivo performances of the ^{99m}Tc and the ^{188}Re conjugates is described.

2. Materials and methods

2.1. Materials

All chemicals were purchased from Aldrich Chemical Co., Sigma or Fluka (Buchs, Switzerland), unless otherwise specified. Rituximab (MabThera) was purchased from Roche, Inc. (F. Hoffmann-La Roche, Ltd., Basel, Switzerland). Pertechnetate [$^{99m}TcO_4^-$] in saline was eluted from a ^{99}Mo/^{99m}Tc generator (Mallinckrodt, Petten, The Netherlands), and perrhenate [$^{188}ReO_4^-$] in saline was eluted from a ^{188}W/^{188}Re generator (ITG, Munich, Germany). For the radiochemical analyses, plasma stability studies and histidine and cysteine challenge, a fast protein liquid chromatography (FPLC) apparatus, Bio-RAD Biologic Duo Flow, equipped with a Berthold HPLC radioactivity monitor CB506 C-1, was employed using a Pharmacia Superose 12 FPLC column (Amersham Biosciences, Dübendorf, Switzerland). The solvent was phosphate buffered saline (PBS) (0.1 M NaCl/0.05 M sodium phosphate buffered, pH 7.4) with 0.05% Tween 20. Ramos and Raji cells were purchased from American Type Culture Collection (Manassas, VA, USA) and female athymic immunodeficient nude mice (CD1-Foxn1^{nu}) were from Charles River, Inc. (Sulzfeld, Germany). All media and additives for cell culture were obtained from BioConcept (Allschwil, Switzerland). For cell experiments and biodistribution studies, the radioactivity was measured with a gamma-counter (Cobra II Packard, Canberra Packard GmbH, Frankfurt, Germany).

2.2. Antibody reduction

Rituximab (10 mg) was reduced with 2-mercaptoethanol (2-ME) (0.7 mmol) to generate free sulfhydryl (–SH) groups. The reaction proceeded at room temperature for 30 min. The reaction mixture was then passed through a PD-10 column (Pharmacia Biotech, Uppsala, Sweden) using PBS (pH 7.4) purged with nitrogen as eluent. Ten fractions of 1 ml were collected. The concentration of the reduced antibody was determined by the measurement of the optical density at 280 nm on a UV/visible spectrophotometer (Perkin Elmer Lambda 35). The number of the resulting free sulfhydryl groups was assayed spectrophotometrically in the presence of the Ellman's reagent at 407 nm. The number of thiol groups was obtained by comparison with a standard curve of

a series of cysteine solutions with concentrations ranging from 0.0125 to 0.1 mM. The results were expressed as sulfhydryl groups per antibody molecule.

2.3. Synthesis of the tricarbonyl precursor $[M(OH_2)_3(CO)_3]^+$ ($M=^{99m}Tc/^{188}Re$)

One milliliter of a $Na[^{99m}TcO_4]$ solution was added to a mixture of 4.5 mg sodium-borano-carbonate, 2.9 mg borax, 9 mg potassium–sodium tartrate tetrahydrate and 7.8 mg sodium carbonate. The solution was heated to 150°C for 40 s in a microwave oven (Initiator Biotage). After cooling, 300 μl of a solution of 0.6 M phosphate buffer/1 M HCl (3:2) was added to adjust the pH to 6.5.

The precursor $[^{188}Re(OH_2)_3(CO)_3^+]$ was prepared according to the following procedure: 1 ml of a $Na[^{188}ReO_4]$ solution was mixed with 50 μl of 4 M HCl, 250 μl of 0.5 M 2-[morpholino]ethanesulfonic acid buffer (MES) and 5 mg of ascorbic acid. The mixture was purged with argon for 10 min and transferred to a 10-ml glass vial that contained 7.5 mg of BH_3NH_3 and had been flushed with CO gas for 20 min and sealed with an aluminum-capped rubber stopper previously. The vial was then incubated at 80°C for 1 h.

2.4. Radiolabeling of the antibody with $^{99m}Tc/^{188}Re(CO)_3$

In a typical radiolabeling experiment, 100 or 250 μg of non-reduced rituximab (RTX_{wt}) or 100, 250 or 500 μg of reduced rituximab (RTX_{red}) in 100 or 150 μl of 0.1 M PBS (pH 7.4) was mixed with 50 or 100 μl (~60 MBq) of a $^{99m}Tc(CO)_3$ solution. The mixture was incubated at 37°C for a period ranging from 30 min to 24 h. The radioimmunoconjugates were used without further purification.

For radiolabeling with ^{188}Re, 100, 250 or 500 μg of RTX_{red} in 100 or 150 μl of 0.1 M PBS (pH 7.4) was mixed with 100 μl (~30 MBq) of a solution of $^{188}Re(CO)_3$. The mixture was reacted under argon at 37°C for a period ranging from 30 min to 24 h. Purification of the radioimmunoconjugate was achieved using a desalting Bio-Spin 6 column (Bio-Rad, Switzerland).

The radiochemical purity was determined using FPLC on a Superose 12 gel filtration column (300 mm, 10 μm) eluting with PBS (pH 7.4) at a flow rate of 1.0 ml/min. The total run time was 35 min and the volume of injection was 50 μl.

2.5. In vitro stability of $^{99m}Tc/^{188}Re(CO)_3$-RTX_{red}

Radiolabeled rituximab was incubated in the presence of cysteine and histidine. In detail, aliquots of 50 μl of $^{99m}Tc/^{188}Re(CO)_3$-RTX_{red} were added to 50 μl of an 80-mM cysteine solution or a 60-mM histidine solution in PBS (pH 7.4). The samples were incubated at 37°C in a thermomixer, and aliquots of 10 μl were removed and analyzed by means of FPLC after 1, 4 and 24 h.

To investigate the stability of the radiolabeled antibodies in human plasma, 50 μl of the $^{99m}Tc/^{188}Re(CO)_3$-RTX_{red} solution was added to 100 μl of human plasma and incubated at 37°C in a thermomixer. Aliquots of 10 μl were removed after 0.5, 1, 4, 6 and 24 h and analyzed by means of FPLC.

2.6. Cell culture

The human Burkitt's lymphoma cell lines Ramos and Raji were used to perform in vitro cell assays and in vivo studies. The cells were cultured in RPMI 1640 medium supplemented with 10% fetal calf serum (FCS), 2 mmol/L of L-glutamine and antibiotics (penicillin 100 IU/ml, streptomycin 100 μg/ml, fungizone 0.25 μg/ml) at 37°C in a humidified atmosphere containing 5% CO_2. For the cell assays and the subcutaneous inoculation of the mice, the cultured cells were washed with cold RPMI 1640 medium and resuspended in cold 0.5% bovine serum albumin (BSA)/PBS (pH 7.4). The concentration of the cells was measured using a haemocytometer slide.

2.7. Immunoreactivity of $^{99m}Tc/^{188}Re(CO)_3$-RTX_{red}

The immunoreactivity was assessed by the method of Lindmo et al. [22] on Raji and/or Ramos cells. Briefly, duplicate samples of a fixed tracer amount of radiolabeled RTX_{red} (5 ng) were incubated with increasing numbers of cells (8×10^4 to 10^7) in a total volume of 550 μl 0.5% BSA/PBS (pH 7.4) on a shaking platform at 37°C for 2 h. Nonspecific binding was determined by parallel duplicate incubations in the presence of 10 μg of the unconjugated antibody. After incubation, cells were separated from the supernatants by centrifugation at 2000×*g* for 5 min. The pellets were washed twice with 0.5% BSA/PBS (pH 7.4), and cell-bound radioactivity was measured with a gamma counter. The data was plotted by total applied radioactivity over specific binding as a function of the inverse cell concentration. The immunoreactive fraction was determined by means of linear extrapolation to infinite cell concentration. Data analysis was performed using GraphPad Prism version 5.0 (GraphPad Software for Science, San Diego, CA, USA).

2.8. Binding affinity of $^{99m}Tc/^{188}Re(CO)_3$-RTX_{red}

Saturation binding experiments with $^{99m}Tc/^{188}Re(CO)_3$-RTX_{red} were performed with Raji and/or Ramos cells by incubating triplicate samples of increasing concentrations of the radioimmunoconjugates (1–3000 ng) with 0.5×10^6 cells suspended in a total volume of 550 μl 0.5% BSA/PBS (pH 7.4) on a shaking platform at 37°C for 2 h. Nonspecific binding was determined by parallel incubations in the presence of 10 μg of the unconjugated antibody. After incubation, cells were separated from the supernatants by centrifugation at 2000×*g* for 5 min. The pellets were washed twice with 0.5% BSA/PBS (pH 7.4), and cell-bound radioactivity was measured with a gamma counter. Data was analyzed using GraphPad Prism version 5.0 and the equilibrium dissociation constant (K_d) and the maximum binding capacity (B_{max}) were estimated.

2.9. In vivo studies of $^{99m}Tc/^{188}Re(CO)_3$-RTX_{red}

The animal studies were conducted in accordance with Swiss Law of Animal Protection. Biodistribution studies were carried out in nude mice. Five-week-old female mice were injected subcutaneously with 5×10^7 Ramos cells in each flank. After the tumors appeared, the animals were used for experiments. The mice were divided into two groups. One group was injected intravenously (tail vein) with $^{99m}Tc(CO)_3$-RTX_{red} (100 μg of antibody, 30 MBq) in 100 μl PBS, while the other group was injected with $^{188}Re(CO)_3$-RTX_{red} (100 μg of antibody, 6 MBq) in 100 μl PBS. Groups of four animals injected with $^{99m}Tc(CO)_3$-RTX_{red} were sacrificed by cervical dislocation at 4, 24 and 48 h after injection. Animals injected with $^{188}Re(CO)_3$-RTX_{red} were sacrificed by cervical dislocation at 4 h (three animals), 24 h (six animals), 48 h and 72 h (four animals each) after injection. Samples of blood and urine were taken, and tumors, normal organs (lung, liver, spleen, stomach, intestine and kidneys), bone and muscle were resected, placed into pre-weighed tubes, weighed and gamma counted. The percentage of injected dose of $^{99m}Tc/^{188}Re(CO)_3$-RTX_{red} per gram of organ (%ID/g) was calculated after correcting for radioactive decay using an aliquot of 10 μl of the injectate.

2.10. Ex vivo autoradiography

For ex vivo autoradiography studies, a nude mouse was injected with $^{188}Re(CO)_3$-RTX_{red} (~8 MBq, 100 μg) and sacrificed 24 h after injection. Immediately after euthanasia, the Ramos tumor xenograft was collected and frozen, embedded in TissueTek (O.C.T. Compound 4583, USA) and stored at −80°C. Frozen tissues were cut into 10-μm sections with a microtome (Bright, Model OFT Instrument Company, Ltd., Huntingdon, England) and mounted on slides (Superfrost, Menzel). The slides were exposed to phosphor imaging screens (super resolution type, 12.5×25.2 cm^2; Perkin Elmer) in X-ray cassettes overnight. The screens were then read by a phosphor imager (Cyclone Plus, Perkin Elmer) to reveal distribution of radioactivity in the sections.

2.11. In vitro autoradiography

After decay of radioactivity, in vitro autoradiography of RTX was performed on sections adjacent to those prepared for ex vivo autoradiography, allowing comparison of CD20 receptor expression and radioactivity distribution in the ex vivo sections. The slides with tissue sections were preincubated in Tris–HCl buffer (170 mM, pH 7.6, with 5 mM $MgCl_2$) with 0.25% (w/v) BSA for 10 min at room temperature. Then, the sections were incubated with 100 μl of a solution of $^{99m}Tc(CO)_3$-RTX_{red} (0.5 MBq/ml in Tris–HCl buffer containing 1% BSA) for 60 min at room temperature. After incubation, the sections were rinsed twice for 5 min in cold Tris–HCl buffer (with 25% BSA), then washed for 5 min in pure Tris–HCl buffer and finally rinsed with cold distilled water. The sections were air-dried and exposed to phosphor imaging screens overnight. The screens were then read by a phophor imager (Cyclone Plus, Perkin Elmer) to reveal distribution of radioactivity in the sections.

3. Results

3.1. Evaluation of non-reduced $^{99m}Tc(CO)_3$-RTX_{wt}

Histidine side chains of proteins have been found to be the preferred sites for labeling with the organometallic ^{99m}Tc tricarbonyl core [20]. We incubated the native non-reduced antibody with $^{99m}Tc(CO)_3$ at 37°C. After 3 h, 30% of the radioactivity was found to be protein bound and at 24 h 70% (data not shown). Varying the amount of the antibody or the reaction volume did only marginally influence the radiolabeling yields. Based on these moderate results obtained with ^{99m}Tc and since previous experience showed that labeling reactions with $^{188}Re(CO)_3$ are slower, it was decided to omit direct labeling experiments with $^{188}Re(CO)_3$ on RTX_{wt}.

3.2. Labeling study of reduced $^{99m}Tc/^{188}Re(CO)_3$-RTX_{red}

Rituximab was reduced with 2-ME to obtain approximately 5±1 –SH groups per protein (n=4) [13,14]. The antibody recovery was 98.5±2.6% (n=4).

The amount of antibody (RTX_{red}) used for radiolabeling with a fixed amount of the $^{99m}Tc(CO)_3$ solution had a significant influence on the labeling yield. Time-dependent radiolabeling studies revealed for ^{99m}Tc almost quantitative incorporation after 3 h at 37°C (98±2%) (Fig. 1), corresponding to a specific activity of 235 MBq/mg of antibody. For radiolabeling with ^{188}Re, the yield increased from 25% after 3 h of incubation at 37°C to a maximum of 83% after 48 h, corresponding to 86 MBq/mg. As virtually all of the ^{99m}Tc was incorporated into the antibody, we used the radioimmunoconjugate without further purification for the in vitro and in vivo studies. In the case of ^{188}Re, the

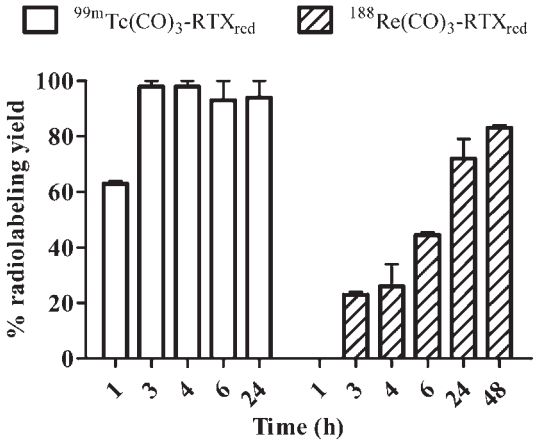

Fig. 1. Effect of reaction time on radiolabeling yields of $^{99m}Tc/^{188}Re(CO)_3$-RTX_{red}.

radiolabeling reactions were separated from unreacted precursor using Bio-Spin desalting columns before further use.

3.3. Cysteine and histidine challenge of $^{99m}Tc/^{188}Re(CO)_3$-RTX_{red}

Amino acid challenges were performed with a 9.5×10^3 M excess of cysteine and 7.4×10^3 M excess of histidine. $^{99m}Tc(CO)_3$-RTX_{red} was susceptible to transchelation in the presence of the strong tridentate ligand systems cysteine and histidine (Fig. 2A). After 1 h, there was only 24% of radiolabeled RTX_{red} remaining when incubated with cysteine, dropping to 5% after 24 h. The radioimmunoconjugates were more stable in the presence of histidine with 81% stability after 1 h and 35% after 24 h.

For pre-purified $^{188}Re(CO)_3$-RTX_{red}, the samples showed to be less susceptible to transchelation. For both cysteine and histidine, more than 90% of radioactivity was protein bound after 24 h (Fig. 2B).

3.4. Plasma stability of $^{99m}Tc/^{188}Re(CO)_3$-RTX_{red}

$^{99m}Tc/^{188}Re(CO)_3$-RTX_{red} revealed no significant reoxidation to pertechnetate or perrhenate when incubated in human plasma at 37°C for 24 h. For $^{99m}Tc(CO)_3$-RTX_{red}, incubation in human plasma caused less than 10% release of $^{99m}Tc(CO)_3$ from the antibody after 24 h (Fig. 3). $^{188}Re(CO)_3RTX_{red}$ remained intact in human plasma up to 24 h and the formation of degradation products was less than 2% (Fig. 3).

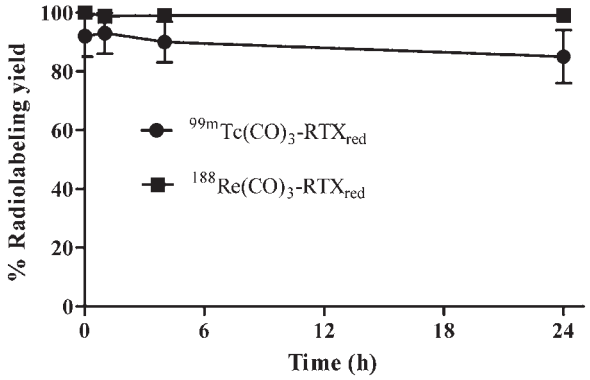

Fig. 3. In vitro stability of $^{99m}Tc/^{188}Re(CO)_3$-RTX_{red} after incubation in human plasma.

3.5. Immunoreactivity and binding affinity of $^{99m}Tc/^{188}Re(CO)_3$-RTX_{red}

The cell binding of the anti-CD20 radioimmunoconjugates was tested with Raji and/or Ramos cells (human B-cell lymphoma lines that express CD20). The immunoreactivities were approximately 50% for $^{99m}Tc(CO)_3$-RTX_{red} (tested with Raji cells) and $^{188}Re(CO)_3$-RTX_{red} (tested with Ramos

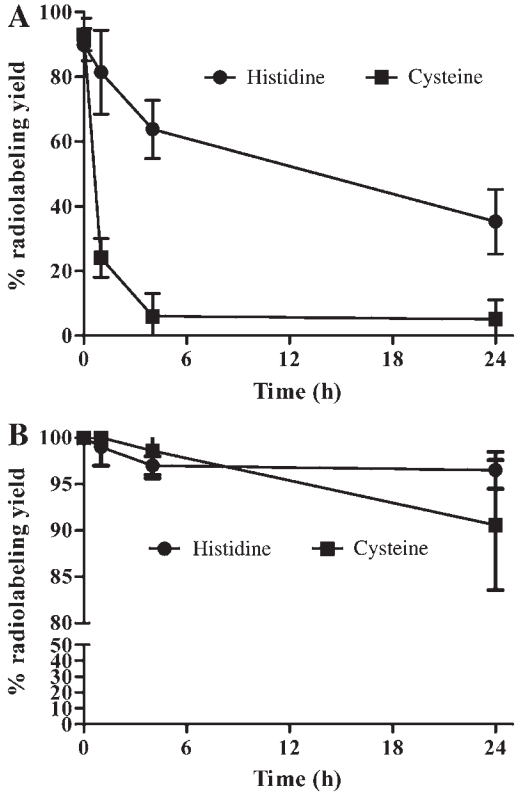

Fig. 2. Displacement of $^{99m}Tc(CO)_3$-RTX_{red} (A) and $^{188}Re(CO)_3$-RTX_{red} (B) in the presence of histidine and cysteine.

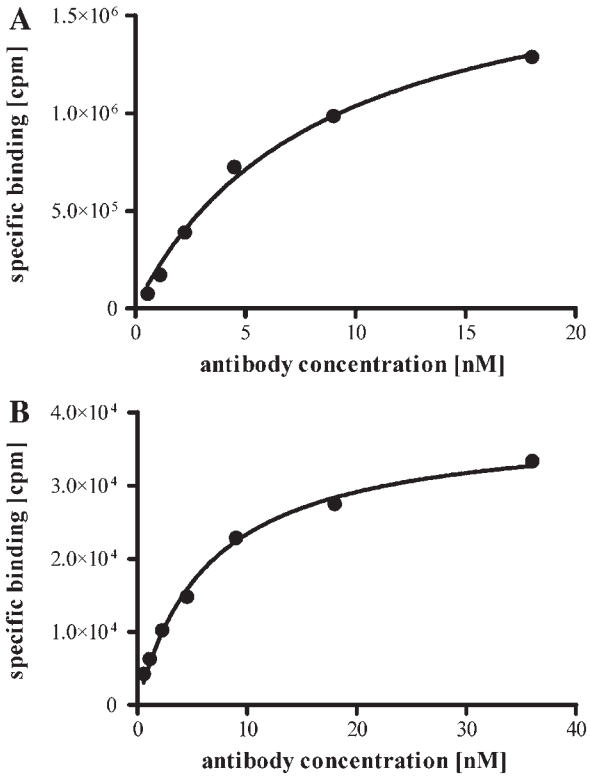

Fig. 4. Saturation binding plot of $^{99m}Tc(CO)_3$-RTX_{red} (A) (K_d=4.7±5.2 nM) and $^{188}Re(CO)_3$-RTX_{red} (B) (K_d=5.7±2.6 nM) to Raji cells.

Table 1
Biodistribution of $^{99m}Tc(CO)_3$-RTX_{red} in nude mice bearing Ramos lymphoma xenografts expressed as the percentage of injected dose per gram (%ID/g)[a]

Organ	4 h	24 h	48 h
Blood	10.9±1.4	2.0±0.2	1.0±0.1
Heart	4.9±0.6	0.9±0.1	0.56±0.04
Lung	6.7±0.6	1.7±0.6	0.84±0.04
Spleen	3.4±0.3	1.1±0.3	0.7±0.1
Kidneys	7.6±0.9	3.6±0.4	2.6±0.4
Stomach	1.5±0.3	0.4±0.2	0.2±0.1
Intestine	1.7±0.2	0.53±0.04	0.3±0.1
Liver	6.4±0.9	2.5±0.2	2.2±0.3
Muscle	0.6±0.1	0.24±0.03	0.16±0.02
Bone	1.4±0.2	0.42±0.03	0.25±0.04
Right tumor	1.0±0.2	0.8±0.5	0.7±0.2
Left tumor	1.0±0.1	0.8±0.6	0.8±0.3
Urine	141.4±77.7	10.3±1.2	4.4±1.6

[a] Values represent the mean±S.D. (n=4) of the %ID/g.

and Raji cells), and 60% for $^{99m}Tc(CO)_3$-RTX_{wt} (tested with Raji cells).

The dissociation constants (K_d) and the binding capacities (B_{max}) of ^{99m}Tc/$^{188}Re(CO)_3$-RTX_{red} were estimated using a saturation binding assay (Fig. 4). Using Raji cells, we found K_d values of 4.7±5.2 nM (n=2) for $^{99m}Tc(CO)_3$-RTX_{red} and 5.7±2.6 nM (n=4) for $^{188}Re(CO)_3$-RTX_{red}. The B_{max} values were 1.3 pmol (188 ng) and 0.73 pmol (109 ng), respectively, which means that approximately 1.5×10^6 and 8.7×10^5 molecules of radiolabeled antibody were bound per cell at saturation. Excellent receptor binding of $^{188}Re(CO)_3$-RTX_{red} was also observed using Ramos cells (5.2±2.9 nM, n=3).

3.6. Biodistribution of ^{99m}Tc/$^{188}Re(CO)_3$-RTX_{red}

The results of the in vivo biodistribution of ^{99m}Tc/$^{188}Re(CO)_3$-RTX_{red} in mice bearing Ramos lymphoma xenografts are shown in Tables 1 and 2. At 4 h postinjection (pi), the radioactivity was mainly located in the blood pool, while the activity of the stomach, muscle, bone and intestine was rather low for both compounds. In both cases, the radioactivity in the liver decreased over time. Maximal tumor accumulation (mean of tumors from both sides) was found after 4 h (1.0 ±0.2 %ID/g) for ^{99m}Tc and after 72 h (2.7±0.6 %ID/g) for ^{188}Re. Radioactivity in the tumors remained almost constant from 24 to 48 h or 72 h pi. Clearance from the blood was fast, leading to increasing tumor-to-blood ratios (Fig. 5) of radioactivity over time (from 0.1 at 4 h after injection to 0.8 at 48 h after injection for ^{99m}Tc and from 0.1 at 4 h after

Table 2
Biodistribution of $^{188}Re(CO)_3$-RTX_{red} in cd1 *nu/nu* mice bearing Ramos lymphoma xenografts expressed as the percentage of injected dose per gram (%ID/g)[a]

Organ	4 h*	24 h**	48 h	72 h
Blood	15.4±2.6	5.8±1.5	3.5±0.4	2.7±0.9
Heart	6.5±0.7	2.7±0.4	1.5±0.2	1.4±0.3
Lung	7.6±1.9	3.9±0.7	2.3±0.3	2.1±0.6
Spleen	4.5±0.8	4.4±2.3	2.6±0.3	3.4±1.1
Kidneys	6.4±0.9	5.8±0.9	4.7±0.5	5.5±0.7
Stomach	0.9±0.2	0.7±0.3	0.3±0.1	0.2±0.1
Intestine	1.5±0.2	1.2±0.6	0.5±0.1	0.6±0.1
Liver	6.6±1.2	5.1±1.0	2.7±0.5	3.1±0.8
Muscle	0.7±0.1	0.7±0.1	0.42±0.04	0.4±0.1
Bone	1.7±0.3	1.4±0.3	0.8±0.1	0.8±0.2
Right tumor	1.2±0.3	2.5±1.7	2.7±0.6	2.5±0.4
Left tumor	1.3±0.4	2.7±1.1	2.2±0.3	2.9±0.9
Urine	5.0±6.4	10.717.4±12.7	11.6±1.2	7.6±3.4

[a] Values represent the mean±S.D. (n=4, n=3*, n=6**) of the %ID/g.

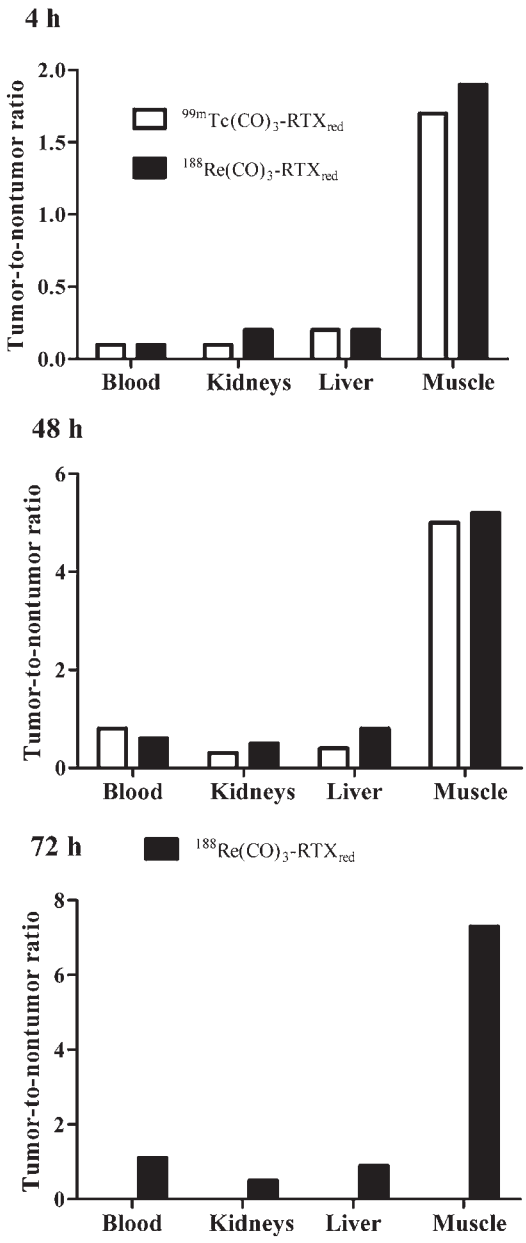

Fig. 5. Tumor-to-normal organ ratios of Ramos xenograft-bearing mice injected either with $^{99m}Tc(CO)_3$-RTX_{red} (□) or with $^{188}Re(CO)_3$-RTX_{red} (■). Tumor-to-normal organ ratios are shown for the radioactivity at 4 and 48 h (^{99m}Tc and ^{188}Re) and at 72 h p.i. (^{188}Re). The values from the left tumor were used for the calculation.

injection to 1.1 at 72 h after injection for ^{188}Re). Significant accumulation of radioactivity was found in the spleen (3.4±0.3 and 4.5±0.8 %ID/g for ^{99m}Tc and ^{188}Re, respectively, 4 h after injection), the kidneys (7.6±0.9 and 6.4±0.9 %ID/g for ^{99m}Tc and ^{188}Re, respectively, 4 h after injection) and the liver (6.4±0.9 and 6.6±1.2 %ID/g for ^{99m}Tc and ^{188}Re, respectively, 4 h after injection).

The postmortem biodistribution data showed that the tumor-to-muscle ratios were already >1 four hours p.i. for both ^{99m}Tc and ^{188}Re. On the other hand, for organs such as liver and kidneys and blood the ratios were <1 even after 48 h. Noticeable differences between unpurified ^{99m}Tc-RTX$_{red}$ and purified ^{188}Re-RTX$_{red}$ could only be observed in the liver and the kidneys after 48 h. The ratio for the other organs (e.g., lung. heart, spleen, stomach) were almost identical for both ^{99m}Tc and ^{188}Re, although the ratios for stomach were higher for ^{188}Re than for ^{99m}Tc.

3.7. Ex vivo and in vitro autoradiography

Poor uptake of the radioimmunoconjugates in the tumors prompted ex vivo autoradiography studies on tumor sections of an animal injected with ^{188}Re(CO)$_3$-RTX$_{red}$. The autoradiography showed that the radioactivity had accumulated primarily on the surface of the tumors, whereas some spots of radioactivity were detected inside the tumor tissue (Fig. 6A). In contrast, when adjacent tumor sections were tested in vitro by adding ^{99m}Tc(CO)$_3$-RTX$_{red}$ after decay of the previously injected radioactivity, a homogenous distribution of CD20 antigen-bound radioactivity throughout the entire tumor tissue was found (Fig. 6B). Blocking experiments with excess cold rituximab showed a complete blockade, and almost no radioactivity was bound to the individual sections (Fig. 6C).

4. Discussion

In the past, three main approaches have been successfully employed for the radiolabeling of antibodies with the matched pair ^{99m}Tc and ^{188}Re, in which the metal is in oxidation state +V: (1) direct labeling, (2) a prelabeling approach and (3) a postlabeling approach [23]. Nevertheless, organometallic technetium and rhenium complexes in low oxidation states have gained considerable attention in the development of novel, target-specific radiopharmaceuticals in the recent years. Tc(I)- and Re(I)-tricarbonyl complexes seem to be a suitable alternative for the labeling of receptor avid proteins. Waibel et al. [20] have established a ^{99m}Tc-labeling technology based on an organometallic chemistry, involving simple mixing of a ^{99m}Tc(I)-carbonyl compound with a His-tagged recombinant protein. Other functionalities in the protein side chains (i.e., carboxylate, primary amines, thiol or thiolate and thioether groups) can also coordinate to the ^{99m}Tc(CO)$_3$ moiety [24]. However, if histidines are available, labeling occurs with high preference at the respective imidazole positions, which is in agreement with investigations of model compounds [25]. Based on this principle, the first radiolabeling approaches in this study were performed using the non-reduced, wild-type rituximab (RTX$_{wt}$). According to the literature, RTX$_{wt}$ comprises 26 histidines [26]. The X-ray structure of the Fab fragment of RTX reveals six histidines [27]. They are not solvent exposed and therefore most likely only poorly accessible by an incoming M(CO)$_3$ core. At the constant Fc part of IgG1s (the subclass of IgGs that RTX belongs to) we identified four solvent-exposed histidines [28]. Furthermore, we localized two regions with four histidines with a 10-Å radius, with one of them exposed to the surface of the protein. It is reasonable to assume that the ^{99m}Tc(CO)$_3$ core coordinates in a mono-

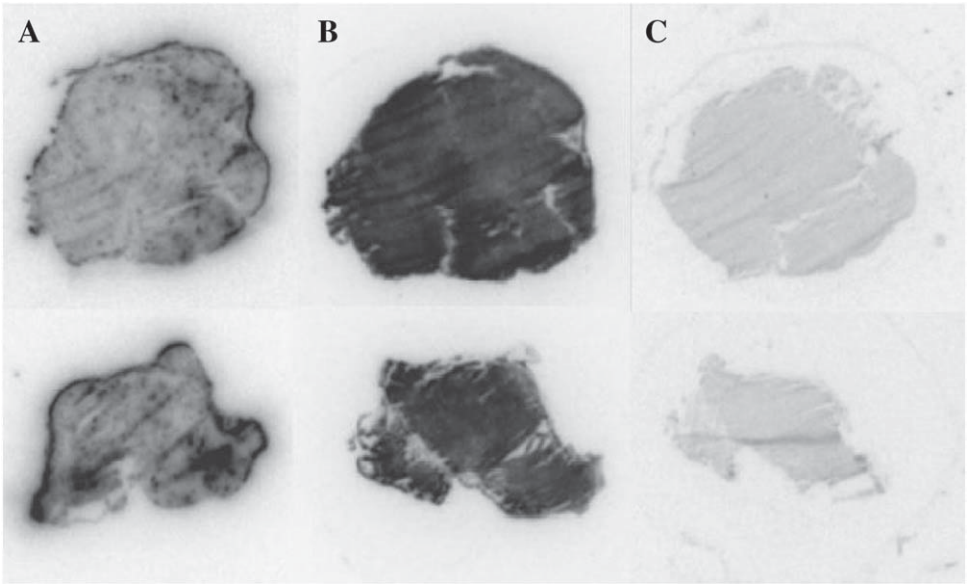

Fig. 6. Ex vivo autoradiogram: section of a tumor after injection of ^{188}Re(CO)$_3$-RTX$_{red}$ (A). In vitro autoradiogram: section of a tumor incubated with ^{99m}Tc(CO)$_3$-RTX$_{red}$ (B) and with ^{99m}Tc(CO)$_3$-RTX$_{red}$ and excess rituximab for CD20 receptor blockade (C).

or polydentate fashion to the protein via these accessible histidine side chains. Particularly, in these histidine-rich regions a bidentate or even a tridentate coordination might be possible after some rearrangement of the side chains around the M(CO)3 core. This situation may be expected to favor a fast and efficient labeling of RTW_{wt} with the $M(CO)_3$ core as observed for, e.g., His-tagged scFv fragments. However, we observed only a very slow (24 h incubation time) and unsatisfactory incorporation of the radioactive precursor into the protein (max. 70% radiolabeling yield after 24 h at 37°C). These results differ from those reported by Chen et al. [21] for the direct labeling of the IgG1 antibody Herceptin (trastuzumab) with $^{188}Re(CO)_3$. They observed a 70% radiolabeling yield with $^{188}Re(CO)_3$ after 24 h at 37°C for 24 h, which was stable in vitro in the presence of human serum albumin or excess histidine for 24 h at room temperature. However, the authors did not characterize and comment on the exact site of labeling of Herceptin. Due to our variable results mentioned above, we did not further test and optimize the direct labeling of RTX_{wt} with ^{188}Re but rather switched to a second strategy. Egli et al. [29] reported some years ago that the preferred amino acids coordinating to the $M(CO)_3$ core follow the series His>Cys>Met>other amino acids. Therefore, we reasoned to increase the numbers of accessible histidine (particularly those of the Fab region) by reducing the native antibody (RTX_{red}). The Fab region of RTX_{wt} comprises five disulfide bonds and a total of 11 cysteines. Additional four disulfide bonds are located in the constant Fc part of an IgG1 and finally the inter-heavy chain disulfide bonds of the hinge region. By reducing the disulfide bonds thiol and thiolate functions are generated, which offer additional, preferred donor groups for the M $(CO)_3$ core.

Antibody reduction is often used for direct radiolabeling as the resulting cysteine residues form stable complexes with $^{99m}Tc/^{188}Re(V)$ [30]. In total, 32 cysteine residues can be obtained by the reduction of IgG1 antibodies [31]. In order to retain the structure of the antibody and to prevent loss of biological activity, we used a mild reduction procedure, yielding an average of five cysteine residues per antibody. Optimized reaction conditions (37°C; 3 h for ^{99m}Tc and 12 h for ^{188}Re) allowed us to radiolabel RTX_{red} with yields of >95% for ^{99m}Tc and approximately 60% for ^{188}Re. Although in the latter case maximal yields were achieved only after 48 h. The differences in reaction rate can be explained by the physicochemical differences between Tc and Re as observed in general and also in particular in the case of the organometallic tricarbonyl core [17]. The optimized reaction time of 12 h for ^{188}Re produced low radiolabeling yields, then a purification procedure was employed using a desalting Bio-Spin6 column to remove the impurities.

The stability of the radiometal complexes was tested in the presence of an excess of free cysteine and histidine. In displacement experiments, $^{188}Re(CO)_3$-RTX_{red} showed only minor dissociation after 24 h. In contrast, we observed substantial loss of protein-bound radioactivity and transchelation of the $^{99m}Tc(CO)_3$ core to cysteine (71±11%) or to histidine (12±7%) after 1 h of incubation at 37°C, respectively. This significant difference in transchelation between the ^{188}Re and the ^{99m}Tc samples can partially be explained by the fact that the ^{188}Re samples were pre-purified before the challenge experiments with histidine and cysteine, whereas the ^{99m}Tc samples were used without purification. Thus, any weakly bound $^{99m}Tc(CO)_3$ cores (e.g., bound via functional groups other than free thiolate groups or histidine) will eventually be stripped from the protein by competing excess of free amino acids and only firmly coordinated ^{99m}Tc $(CO)_3$ cores (presumably bi- or tridentately) are inert against displacement. This is a reasonable explanation since during purification of the ^{188}Re samples 50% of the initial radioactivity is also lost or stripped during the desalting step. Another possible explanation is that the kinetics for ^{99m}Tc labeling is faster, providing at the same time weaker binding to the antibody compared to ^{188}Re labeling. On the other hand, the differences in human plasma stability were less pronounced (85% for ^{99m}Tc vs. 99% for ^{188}Re, 24 h post incubation at 37°C).

Binding affinity studies showed that $^{99m}Tc(CO)_3$-RTX_{red} and $^{188}Re(CO)_3$-RTX_{red} had excellent receptor binding, K_d=5 and 6 nM, respectively, which is in good agreement with the published value of 5.0 nM [10]. The biodistribution of ^{99m}Tc and ^{188}Re-radiolabeled rituximab was studied in nude mice bearing subcutaneous Ramos lymphoma xenografts, an established tumor model [32]. The blood clearance of $^{99m}Tc(CO)_3$-RTX_{red} was faster in comparison to ^{188}Re $(CO)_3$-RTX_{red} (10.9 %ID/g at 4 h pi to 1.0 %ID/g at 48 h pi and 15.4 %ID/g at 4 h pi to 2.7 %ID/g at 72 h pi, respectively). The increased circulation time in blood presumably explains the higher tumor uptake for ^{188}Re $(CO)_3$-RTX_{red}. Furthermore, while the mean tumor (mean of tumors from both sides) uptake of $^{188}Re(CO)_3$-RTX_{red} increased from 1.3 %ID/g at 4 h pi to 2.7 %ID/g at 72 h pi, it decreased from 1.0 %ID/g at 4 h pi to 0.7 %ID/g at 48 h pi for $^{99m}Tc(CO)_3$-RTX_{red}. We do not have a conclusive explanation for the faster tumor washout in the case of ^{99m}Tc. The low tumor uptake of both conjugates might be ascribed to the large tumor sizes. In this study, the subcutaneous Ramos xenografts reached a mass up to 3 g. It is well known that penetration of solid tumors by antibodies is slow and dependent on the vascularization of malignant tissues [33,34]. To evaluate tumor penetration, we performed ex vivo autoradiography of tumor sections of animals injected with $^{188}Re(CO)_3$-RTX_{red}. As expected, the autoradiography clearly indicated that the radioactivity accumulated primarily on the outer rim of the xenografts, thus proving poor penetration. We therefore suggest using subcutaneous Ramos xenografts of much smaller sizes in order to obtain higher values of uptake of the radioimmunoconjugates. Nonspecific uptake of radioactivity into the excretion organs (liver and kidneys) did not differ among the compounds and was comparable to the results described in the literature for RTX_{red} labeled with Re(V)

[13]. The high uptake of radioactivity into the lungs and the spleen is often observed with anti-CD20 antibodies and can be explained by the accumulation of antigen-expressing B lymphocytes in these organs [35]. Given that we did not observe accumulation of radioactivity in the stomach for both compounds, we can conclude that neither $^{99m}TcO_4^-$ nor $^{188}ReO_4^-$ was formed in significant amounts.

To assess the tumor-to-non-tumor ratios, we chose the muscle as an internal reference. For $^{99m}Tc(CO)_3$-RTX_{red}, the ratio of tumor to muscle was 1.7 at 4 h pi and increased to 4.0 at 24 h pi. For $^{188}Re(CO)_3$-RTX_{red}, we observed a tumor-to-muscle ratio of 1.8 at 4 h pi, increasing to 6.8 at 72 h pi.

5. Conclusion

An alternative route for the direct radiolabeling of the anti-CD20 mAb rituximab with both ^{99m}Tc and ^{188}Re using the tricarbonyl technique was developed and assessed. Acceptable radiolabeling yields could only be achieved after reduction of the antibody. Unfortunately, the exact site and mode of coordination of the $M(CO)_3$ core are not clear. It can only be speculated but not proven at this time whether the metal core is primarily coordinated via the newly accessible histidines of the Fab portion (after a moderate unfolding of the tertiary protein structure as a consequence of reduction of the disulfide bonds) or in fact via the newly available cysteine side chains (or a combination of both). One also has to keep in mind that RTX_{red} per se represents a heterogeneous product, since the number and site of reduced disulfide bonds vary. Thus, also $M(CO)_3$-RTX_{red} is presumably a heterogeneous mixture of different species. In vitro binding studies revealed full retention of biological activity for both ^{99m}Tc and ^{188}Re immunoconjugates. Both $^{99m}Tc(CO)_3$-RTX_{red} and $^{188}Re(CO)_3$-RTX_{red} revealed an almost similar pharmacokinetic profile in vivo. However, the radiolabeling procedure of the reduced antibody with ^{188}Re needs further improvement to consider these radioimmunoconjugates as a suitable alternative to the $^{111}In/^{90}Y$-Zevalin system. Notably, the necessity of reduction of the antibody and the long incubation time to achieve reasonable radiolabeling yields is prohibitive for a convenient application of this approach in a clinical environment.

Acknowledgment

The National Council of Technological and Scientific Development (Conselho Nacional de Desenvolvimento Científico e Tecnológico – CNPq/Brazil) is greatly acknowledged for granting a fellowship to C.R. Dias.

References

[1] Hamoudeh M, Kamleh MA, Diab R, Fessi H. Radionuclides delivery systems for nuclear imaging and radiotherapy of cancer. Adv Drug Deliv Rev 2008;60:1329–46.

[2] Hernandez MC, Knox SJ. Radiobiology of radioimmunotherapy: targeting CD20 B-cell antigen in non-Hodgkin's lymphoma. Int J Rad Oncol Biol Phys 2004;59(5):1274–87.

[3] Cheson BD. Radioimmunotherapy of non-Hodgkin lymphomas. Blood 2003;101(2):391–8.

[4] Conti PS. Radioimmunotherapy with yttrium 90 ibritumomab tiuxetan (Zevalin): the role of the nuclear medicine physician. Semin Nucl Med 2004;34:2–3.

[5] Macklis RM. Radioimmunotherapy as a therapeutic option for non-Hodgkin's lymphoma. Semin Radiat Oncol 2007;17:176–83.

[6] Kosmas C, Stamatopoulos K, Stavroyianni N, Tsavaris N, Papadaki T. Anti-CD20-based therapy of B cell lymphoma: state of the art. Leukemia 2002;16:2004–15.

[7] Eisenberg R, Looney RJ. The therapeutic potential of anti-CD20 What do B-cells do? Clin Immunol 2005;117:207–13.

[8] Liebenguth P, Temple SV. Radioimmunotherapy for non-Hodgkin's lymphoma. Semin Oncol Nursing 2006;22(4):257–66.

[9] Rao AV, Schmader K. Monoclonal antibodies as targeted therapy in hematologic malignancies in older adults. Am J Geriatric Pharmacoth 2007;5(3):247–62.

[10] Maloney DG, Grillo-López AJ, White CA, Bodkin D, Schilder RJ, Neidhart JA, et al. IDEC-C2B8 (Rituximab) anti-CD20 monoclonal antibody therapy in patients with relapsed low-grade non-Hodgkin's lymphoma. Blood 1997;90:2188–95.

[11] Stern M, Herrmann R. Overview of monoclonal antibodies in cancer therapy: present and promise. Critical Rev Oncol Hematol 2005;54: 11–29.

[12] Müller C, Schubiger PA, Schibli R. Isostructural folate conjugates radiolabeled with the matched pair $^{99m}Tc/^{188}Re$: a potential strategy for diagnosis and therapy of folate receptor-positive tumors. Nucl Med Biol 2007;34(6):595–601.

[13] Ferro-Flores G, Torres-García E, García-Pedroza L, Arteaga de Murphy C, Pedraza-López M, Garnica-Garza H. An efficient, reproducible and fast preparation of ^{188}Re-anti-CD20 for the treatment of non-Hodgkin's lymphoma. Nucl Med Comm 2005;26: 793–9.

[14] Stopar TG, Mlinaric-Rascan I, Fettich J, Hojker S, Mather SJ. ^{99m}Tc-Rituximab radiolabelled by photo-activation: a new non-Hodgkin's lymphoma imaging agent. Eur J Nucl Med Mol Imaging 2006;33 (1):53–9.

[15] Torres-García E, Ferro-Flores G, Arteaga de Murphy C, Correa-González L, Pichardo-Romero PA. Biokinetics and dosimetry of ^{188}Re-anti-CD20 in patients with non-Hodgkin's lymphoma: preliminary experience. Arch Med Res 2008;39(1):100–9.

[16] Raposinho PD, Correia JDG, Alves S, Botelho MF, Santos AC, Santos I. A $^{99m}Tc(CO)_3$-labeled pyrazolyl-[alpha]-melanocyte-stimulating hormone analog conjugate for melanoma targeting. Nucl Med Biol 2008;35(1):91–9.

[17] Schibli R, Schwarzbach R, Alberto R, Ortner K, Schmalle H, Dumas C, et al. Steps toward high specific activity labeling of biomolecules for therapeutic application: preparation of precursor $[^{188}Re(H_2O)_3(CO)_3]^+$ and synthesis of tailor-made bifunctional ligand systems. Bioconjugate Chem 2002;13:750–6.

[18] Deyev SM, Waibel R, Lebedenko EN, Schubiger AP, Plückthun A. Design of multivalent complexes using the barnase–barstar module. Nat Biotechnol 2003;21(12):1486–92.

[19] Willuda J, Kubetzko S, Waibel R, Schubiger PA, Zangemeister-Wittke U, Plückthun A. Tumor targeting of mono-, di-, and tetravalent anti-p185 (HER-2) miniantibodies multimerized by self-associating peptides. J Biol Chem 2001;276(17):14385–92.

[20] Waibel R, Alberto R, Willuda J, Finnern R, Schibli R, Stichelberger A, et al. Stable one-step technetium-99m labeling of His-tagged recombinant proteins with a novel Tc(I)–carbonyl complex. Nat Biotechnol 1999;17:897–901.

[21] Chen KT, Lee TW, Lo JM. In vivo examination of $^{188}Re(I)$-tricarbonyl-labeled trastuzumab to target HER2-overexpressing breast cancer. Nucl Med Biol 2009;36:355–61.

[22] Lindmo T, Boven E, Cuttitta F, Fedorko J, Bunn PA. Determination of the immunoreactive function of radiolabeled monoclonal antibodies by linear extrapolation to binding at infinite antigen excess. J Immunol Methods 1984;72(1):77–89.
[23] Liu S. Bifunctional coupling agents for radiolabeling of biomolecules and target-specific delivery of metallic radionuclides. Adv Drug Del Rev 2008;60(12):1347–70.
[24] Alberto R, Schibli R, Waibel R, Abram U, Schubiger AP. Basic aqueous chemistry of $[M(OH_2)_3(CO)_3]^+$ (M=Re, Tc) directed towards radiopharmaceutical application. Coord Chem Rev 1999;192:901–19.
[25] Amann A, Decristoforo C, Ott I, Wenger M, Bader D, Alberto R, et al. Surfactant protein B labelled with $[^{99m}Tc(CO)_3(H_2O)_3]^+$ retains biological activity in vitro. Nucl Med Biol 2001;28(3):243–50.
[26] The Drug Bank database: http://www.drugbank.ca/drugs/DB00073.
[27] Du J, Wang H, Zhong C, Peng B, Zhang M, Li B, et al. Structural basis for recognition of CD20 by therapeutic antibody rituximab. J Biol Chem 2007;282(20):15073–80.
[28] DeLano WL, Ultsch MH, de Vos AM, Wells JA. Convergent solutions to binding at a protein-protein interface. Science 2000;287(5456): 1279–83.
[29] Egli A, Alberto R, Tannatoli L, Schibli R, Abram U, Schaffland A, et al. Organometallic ^{99m}Tc-Aquaion labels peptide to an unprecedented high specific activity. J Nucl Med 1999;40:1913–7.
[30] Eckelman WC, Steigman J. Direct labeling with ^{99m}Tc. Nucl Med Biol 1991;18:3–7.
[31] Salfeld JG. Isotype selection in antibody engineering. Nat Biotech 2007;25:1369–72.
[32] Subbiah K, Hamlin DK, Pagel JM, Wilbur DS, Meyer DL, Axworthy DB, et al. Comparison of immunoscintigraphy, efficacy, and toxicity of conventional and pretargeted radioimmunotherapy in CD20-expressing human lymphoma xenografts. J Nucl Med 2003;44: 437–45.
[33] DeNardo SJ, Kroger LA, DeNardo GL. A new era for radiolabeled antibodies in cancer? Curr Opin Immunol 1999;11 (5):563–9.
[34] Holliger P, Hudson PJ. Engineering antibody fragments and the rise of single domains. Nat Biotech 2005;23:1126–36.
[35] Jalilian AR, Mirsadeghi L, Haji-Hosseini R, Khorrami A. Preparation, quality control and biodistribution studies of [^{67}Ga]-DOTA-anti-CD20. Radiochim Acta 2008;96:167–74.